Preexisting human antibodies neutralize recently emerged H7N9 influenza strains

Carole J. Henry Dunand,[1] Paul E. Leon,[2,3] Kaval Kaur,[1,4] Gene S. Tan,[2] Nai-Ying Zheng,[1] Sarah Andrews,[1] Min Huang,[1] Xinyan Qu,[1] Yunping Huang,[1] Marlene Salgado-Ferrer,[1] Irvin Y. Ho,[1] William Taylor,[1] Rong Hai,[2] Jens Wrammert,[5] Rafi Ahmed,[5] Adolfo García-Sastre,[2,6,7] Peter Palese,[2,6] Florian Krammer,[2] and Patrick C. Wilson[1,4]

[1]Department of Medicine, Section of Rheumatology, Gwen Knapp Center for Lupus and Immunology Research, The University of Chicago, Chicago, Illinois, USA. [2]Department of Microbiology and [3]Graduate School of Biomedical Sciences, Icahn School of Medicine at Mount Sinai, New York, New York, USA. [4]Committee on Immunology, The University of Chicago, Chicago, Illinois, USA. [5]Emory Vaccine Center, Department of Microbiology and Immunology, Emory University School of Medicine, Atlanta, Georgia, USA. [6]Department of Medicine and [7]Global Health and Emerging Pathogens Institute, Icahn School of Medicine at Mount Sinai, New York, New York, USA.

The emergence and seasonal persistence of pathogenic H7N9 influenza viruses in China have raised concerns about the pandemic potential of this strain, which, if realized, would have a substantial effect on global health and economies. H7N9 viruses are able to bind to human sialic acid receptors and are also able to develop resistance to neuraminidase inhibitors without a loss in fitness. It is not clear whether prior exposure to circulating human influenza viruses or influenza vaccination confers immunity to H7N9 strains. Here, we demonstrate that 3 of 83 H3 HA-reactive monoclonal antibodies generated by individuals that had previously undergone influenza A virus vaccination were able to neutralize H7N9 viruses and protect mice against homologous challenge. The H7N9-neutralizing antibodies bound to the HA stalk domain but exhibited a difference in their breadth of reactivity to different H7 influenza subtypes. Mapping viral escape mutations suggested that these antibodies bind at least two different epitopes on the stalk region. Together, these results indicate that these broadly neutralizing antibodies may contribute to the development of therapies against H7N9 strains and may also be effective against pathogenic H7 strains that emerge in the future.

Introduction

Influenza A viruses evade the human immune system by changing the antigenic regions of their surface glycoproteins using two mechanisms: antigenic drift (point mutations) and antigenic shift (gene segment reassortments) (1). Antigenic variation is further increased by divergent evolution, as influenza virus strains recirculate continually among different host reservoirs, especially humans and avian species. The HA glycoprotein is the main target of neutralizing antibodies and is composed of an immunodominant globular head domain and a stalk domain (2). HA subtypes are classified into two groups based on their antigenic properties: amino acid sequences and structural features (3). Group 2 influenza A viruses include the H3 subtype, which further contains the seasonal H3N2 human strains, and the H7 subtype, which contains highly pathogenic avian influenza A viruses (4). Previously, infections with H7 viruses, through exposure to poultry, generally resulted in uncomplicated influenza illness and/or mild conjunctivitis (demonstrated for H7N3), with only one fatal case observed during an outbreak in The Netherlands (H7N7) (5, 6). However in 2013, a novel influenza A virus (H7N9), the product of genetic reassortment of various avian strains, emerged in China. This virus, associated with a high frequency of fatal human disease, appeared to have a wide dispersion and the potential for human-to-human transmission (7–12). Although the virus received the most publicity in 2013 (a year with 153 cases), the H7N9 virus shows a seasonal pattern, with most infections occurring during the winter season. The incidence of infection continues to increase, with nearly twice as many new H7N9 infections (301 cases) reported in 2014, totaling 454 cases, according to the World Health Organization, as of July 2014. These cases occurred in 12 provinces of China, with imported cases in Malaysia and Taiwan. The incidence of H7N9 infection combined with its abilities to bind to human receptor orthologs and to develop resistance to neuraminidase inhibitors without fitness loss has raised concerns about the pandemic potential of the H7N9 virus (13–15). With H7 strains currently posing a threat to human health, it is important to determine whether there is cross-protection generated from group 2 influenza virus vaccinations. Over several years, we have generated human antibodies from plasmablasts of volunteers vaccinated with the seasonal influenza virus vaccine (refs. 16, 17, and our unpublished data). Because plasmablasts are activated during an ongoing immune response, this allows us to determine whether prior vaccination, especially with H3N2 strains, induced cross-reactive antibodies that neutralize H7 strains. Given the lack of a vaccine against novel H7 viruses, the isolation and characterization of monoclonal antibodies with neutralizing activity can direct vaccine design and also provide a therapeutic resource.

Results

Cross-reactive antibodies induced by past influenza A virus exposure react with novel pathogenic H7N9 strains. To identify H7-binding antibodies, we developed an antibody microarray technology that

Authorship note: Patrick C. Wilson and Florian Krammer contributed equally to this work.
Conflict of interest: The authors have declared that no conflict of interest exists.
Submitted: July 21, 2014; **Accepted:** January 6, 2015.
Reference information: *J Clin Invest*. 2015;125(3):1255–1268. doi:10.1172/JCI74374.

allows high-throughput screening for cross-reactivity to influenza HA proteins (Figure 1A). We selected 83 antibodies, from 28 individuals, that were previously detected as H3N2 reactive by ELISA and tested their reactivity to different H3 and H7 recombinant HAs. We report here that 6 of the 83 (7%) H3-reactive antibodies bind both the A/Shanghai/1/2013 (H7N9) and A/Anhui/1/2013 (H7N9) strains isolated from the first infected patients in China. These 6 antibodies were each from different individuals, thus 21% (6 of 28 individuals) of this cohort had evidence of H7 cross-reactive immunity. Since we screened an average of only 3 H3N2-reactive antibodies per subject, we predict that a higher percentage of people previously vaccinated with H3N2 strains are likely to have cross-reactive antibodies that bind to the novel H7N9 strains.

To assess more comprehensively the frequency of cross-reactive immunity within the vaccinated population, we analyzed the frequency of H3/H7-reactive memory cells 14 days after seasonal vaccination in 13 individuals by ELISPOT. Since cross-reactive antibodies typically bind to conserved epitopes on the stalk domain, we determined the percentage of H7 stalk–reactive memory cells by using a chimeric HA, which is composed of the stalk domain of the A/Shanghai/1/2013 (H7N9) strain and the globular head domain of an H4 strain (A/duck/Czechoslovakia/1956 [H4N6]), to which humans are naive (18). Two control HAs were used: one composed of the globular head region of the H4 strain and one composed of the globular head region of the A/Shanghai/1/2013 (H7N9) strain. The reactivity of memory cells to H3 was assessed using commercially available H3 HAs. Using this method, 9% (median 9.3%, range 4.9%–15.9%) of H3N2 HA-reactive IgG memory cells bound to the H7 stalk. This suggests that, out of the H3N2-specific memory cells generated from seasonal vaccinations, 9% are group 2 cross-reactive (Figure 1B). Collectively, our antibody microarray and ELISPOT results demonstrate that at least 7% of H3N2-reactive B cells react with H7 influenza strains.

Three of the cross-reactive antibodies neutralize pathogenic H7N9 strains in vitro and protect mice from lethal infection. To determine the functional capacity of our H7 cross-reactive antibodies, we assessed their ability to neutralize the A/Shanghai/1/2013 virus in a standard microneutralization assay. Three of the six cross-reactive antibodies neutralized the H7N9 virus in vitro (045-051310-2B06, 042-100809-2F04, and S6-B01), whereas a human IgG control antibody did not (Figure 1C). S6-B01 and 042-100809-2F04 were induced by the seasonal vaccine H3N2 strains A/Wisconsin/67/2005 and A/Uruguay/716/2007, respectively (Supplemental Table 1; supplemental material available online with this article; doi:10.1172/JCI74374DS1). The antibody 045-051310-2B06 was generated in response to the pandemic A/California/04/2009 (H1N1) strain. 045-051310-2B06 also bound the A/Uruguay/716/2007 (H3N2) strain, and all 3 neutralizing antibodies bound various H7 strains (Supplemental Figure 1).

Because in vitro neutralization is not always predictive of in vivo potency (19), we tested the protective efficacy of the 3 H7N9-neutralizing antibodies in a mouse model. Mice were treated prophylactically with 1.5, 5, or 15 mg/kg of each antibody intraperitoneally and then challenged with a lethal dose (7.5 LD_{50}) of A/Shanghai/1/2013 virus (H7N9). In this model, the 3 antibodies showed comparable efficacy, as they conferred protection at the lowest dose of 1.5 mg/kg, with all mice in each group surviving infection. Although mice were protected from mortality at a dose of 1.5 mg/kg 042-100809-2F04, 1 of 5 mice treated with 5 mg/kg of antibody showed weight loss of about 25%. Untreated control mice and those treated with 15 mg/kg polyclonal human IgG lost weight and succumbed to infection by day 8 to 9. Furthermore, mice treated with an H3N2-neutralizing antibody that did not bind H7 (011-10069 2C01) did not survive past day 8–9 (Figure 2A and Supplemental Figure 2A). These antibodies were also tested in a therapeutic model, with 15 mg/kg of each antibody being administered 24 hours after infection to the respective groups. All 3 antibodies were able to protect mice from the lethal challenge. A similar experiment was conducted with the antibody being delivered 72 hours after infection, and we observed 100% survival only with 042-100809-2F04. For the 045-051310-2B06 and S6-B01 antibodies, reduced survival, 80% and 60%, respectively, was observed (Figure 2B and Supplemental Figure 2B). These findings demonstrate that human antibodies induced by vaccination that bind H3N2 influenza virus strains infectious to humans can provide in vivo protection of mice against lethal infections with the pathogenic H7N9 influenza virus.

The cross-reactive antibodies neutralize various influenza strains. These H7-neutralizing antibodies are predicted to bind epitopes conserved among a wide variety of influenza strains. Therefore cross-reactivity to multiple influenza A group 1 (H1 and H5) and group 2 (H3, H7, and H15) recombinant HAs was assessed. 045-051310-2B06, 042-100809-2F04, and S6-B01 bound at low concentration to various H3N2 and H7 strains as well as the H15N9 strain, confirming their cross-reactivity within group 2 (Figure 3). The antibodies bound H7 strains from both the North American and Eurasian lineages (phylogenetic tree, Supplemental Figure 3), suggesting cross-protection will also exist against other potentially emerging avian H7 strains (20). 042-100809-2F04 bound only to group 2 HAs. Not surprisingly, 045-051310-2B06 bound the A/California/04/2009 H1N1 strain at low concentration but also cross-reacted with various H1N1 strains. Interestingly, S6-B01 also bound to H1N1 strains, and both 045-051310-2B06 and S6-B01 cross-reacted with the A/Vietnam/1203/2004 (H5N1) HA (Figure 3). None of the H7-neutralizing antibodies bound to influenza B HA of either the Yamagata or Victoria lineage (data not shown). Thus, these 3 antibodies displayed unique strain specificities.

To assess the breadth of neutralization capacity of these antibodies, we performed plaque reduction assays with various influenza virus strains (Figure 4A). 045-051310-2B06 and 042-100809-2F04 were able to prevent infection of MDCK cells, with similar efficacy for all of the H3N2 strains tested ($PRNT_{50}$ ranging from 6 to 19 μg/ml). Furthermore, both of these antibodies neutralized A/Shanghai/1/2013 (H7N9) but at a higher concentration when compared with that required for neutralization of H3N2 strains ($PRNT_{50}$ = 19 μg/ml for 045-051310-2B06 and $PRNT_{50}$ = 27 μg/ml for 042-100809-2F04). 045-051310-2B06 also showed neutralization efficacy against the A/chicken/Jalisco/12283/12 (H7N3) strain from the North American lineage ($PRNT_{50}$ = 18 μg/ml). S6-B01 potently neutralized all H3N2 and H7 strains at low concentrations ($PRNT_{50}$ ranging from 3 to 6 μg/ml). 045-051310-2B06 neutralized the A/California/04/2009 (H1N1) strain ($PRNT_{50}$ = 5.5 μg/ml), whereas S6-B01 did not ($PRNT_{50}$ > 120 μg/ml). This demonstrates that 042-100809-2F04 is a group

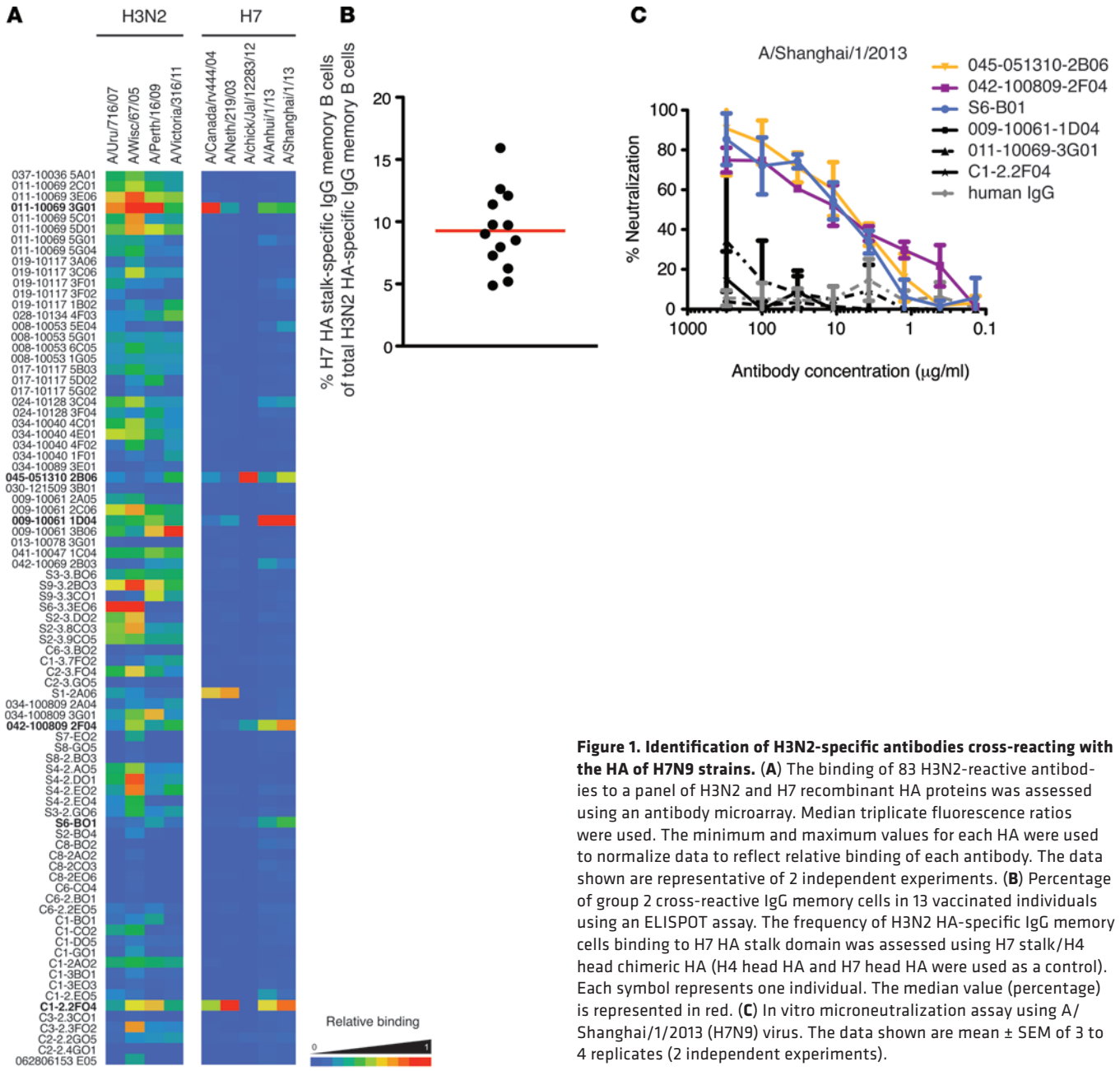

Figure 1. Identification of H3N2-specific antibodies cross-reacting with the HA of H7N9 strains. (**A**) The binding of 83 H3N2-reactive antibodies to a panel of H3N2 and H7 recombinant HA proteins was assessed using an antibody microarray. Median triplicate fluorescence ratios were used. The minimum and maximum values for each HA were used to normalize data to reflect relative binding of each antibody. The data shown are representative of 2 independent experiments. (**B**) Percentage of group 2 cross-reactive IgG memory cells in 13 vaccinated individuals using an ELISPOT assay. The frequency of H3N2 HA-specific IgG memory cells binding to H7 HA stalk domain was assessed using H7 stalk/H4 head chimeric HA (H4 head HA and H7 head HA were used as a control). Each symbol represents one individual. The median value (percentage) is represented in red. (**C**) In vitro microneutralization assay using A/Shanghai/1/2013 (H7N9) virus. The data shown are mean ± SEM of 3 to 4 replicates (2 independent experiments).

2 broadly neutralizing antibody, whereas 045-051310-2B06 is a pan–influenza A–neutralizing antibody (both group 1 and 2). S6-B01 binds group 1 and 2 strains, but in vitro neutralization is only detected among group 2 viruses.

The neutralizing cross-reactive antibodies bind to conserved but distinct epitopes on the HA stalk domain. The majority of neutralizing antibodies generated after exposure to influenza viruses are strain specific, binding the highly variable loops on the globular head domain of HA. On the other hand, broadly neutralizing monoclonal antibodies (group 1 and 2) often bind conserved epitopes on the HA stalk domain. Antibodies that bind the head generally have hemagglutination inhibition (HI) activity, whereas antibodies that bind to the stalk domain of HA do not but neutralize by post-entry mechanisms of inhibition (21, 22). The H7N9-neutralizing antibodies herein showed no HI activity against any tested strain (data not shown). Moreover, competitive inhibition using CR9114, a previously described stalk-reactive antibody (19), suggested that the epitopes targeted by the 3 antibodies are within the stalk domain of HA (Figure 4B). As expected, 009-10061-1D04, an antibody that displays HI activity (Figure 4C) and binds to H3N2 and H7 strains (Figure 1A), was not inhibited by any of the stalk antibodies tested (Figure 4B).

To further map the epitopes targeted by the 3 neutralizing antibodies, we generated escape mutants of the A/Shanghai/1/2013 (H7N9) virus. It is postulated that, under antibody pressure, viruses undergo mutations at sites that are targeted by the antibody and this allows the identification of the binding site. We sequenced 4 escape mutants for each antibody and analyzed

Table 1. Mutations displayed by the escape mutants

Antibodies	Head mutations	Stalk mutations
045-051310-2B06	G195E	V318I I384N
042-100809-2F04	G63E G234D	R364K
S6-B01	A198E G214E	I384T

the mutations. The same virus passaged in absence of antibody was used as a control. All 4 clones for each antibody displayed the same mutations. None of the mutations were found with the virus passaged without antibody, suggesting that the mutations were a result of the antibody pressure. A total of 3 amino acid substitutions were identified for each antibody in the HA segment (Table 1). Interestingly, we observed mutations both in the stalk and the head domains. The escape mutant generated with the antibody 045-051310-2B06 displayed two mutations in the stalk region, V318I and I384N (H7 numbering starting with methionine), and one in the globular head region, G195E. The escape mutant generated with the antibody S6-B01 displayed one mutation in the stalk region, I384T. This mutation arose at the same residue as the escape mutant generated by 045-051310-2B06, but the substitution was different. Both mutations at this residue were located in the conserved epitope targeted by CR9114 (19). Two mutations in the globular head, A198E and G214E, were also found. Finally, the escape mutant generated with the antibody 042-100809-2F04 displayed one mutation in the stalk region, R364K, and two in the globular head region, G63E and G234D. The stalk mutation was located in the conserved epitope targeted by CR8020, a group 2–neutralizing antibody (23).

Escape-mediated loss of binding is complete for 045-051310-2B06 and 042-100809-2F04 but not for S6-B01. To test the effect of the mutations on antibody binding, we infected MDCK cells with the original virus (A/Shanghai/1/2013) or the different escape mutant viruses and assessed the binding of each antibody to the cells by immunofluorescence (Figure 5). 045-051310-2B06 had no detectable binding when the cells were infected with its corresponding escape mutant, suggesting that the mutations affect antigenicity (24). In addition, there was no binding for 045-051310-2B06 to the escape mutant generated from S6-B01. Interestingly, for the S6-B01 antibody, binding to both of these escape mutants was only partially lost. Finally, the 042-100809-2F04 antibody lost binding to its own escape mutant but not to the escape mutants generated from the other two antibodies. These results confirm that the neutralizing cross-reactive antibodies bind to two different epitopes on the HA stalk domain.

To determine the role of the head versus the stalk domain mutations, we expressed different variants of the mutated recombinant HAs. For each of the 3 escape mutants, we generated two HAs and assessed antibody binding by ELISA; the first HA incorporated the mutations in both the head and the stalk domains, while the second HA incorporated only the stalk mutations with a wild-type globular head domain. We observed reduced binding to both mutated HAs for the antibody 045-051310-2B06 (Figure 6). However, the loss of binding was more dramatic with the stalk-only mutated HA, suggesting that the stalk mutations are antigenic mutations. The same pattern of binding was detected when CR9114 was tested with the 045-051310-2B06 HA variants. In line with the immunofluorescence observations, a slightly reduced binding was seen with the fully mutated HAs for S6-B01. However, there was no reduction in binding to the stalk-only mutated HA. This finding was confirmed using CR9114, which has the same footprint as 045-051310-2B06 and S6-B01. Therefore, although these mutations mediate viral escape from neutralization by the antibody, they do not ablate antibody binding. Finally, 042-100809-2F04 showed reduced binding to its own HA mutants (both mutated stalk-only and fully mutated HAs). But the loss of binding was more dramatic when both the head and the stalk mutations were present. This was confirmed with CR8020, which has the same footprint as 042-100809-2F04.

Escape mutant viruses have diminished pathogenicity in vivo. To evaluate the importance of the stalk mutations in the loss of viral fitness, we generated infectious reassortant viruses with these mutations for each of the 3 antibodies and determined the LD_{50} of the different viruses in mice. Experiments were conducted with different challenge doses, ranging from 100 to 100,000 PFU per mouse. Although the 045-051310-2B06 and S6-B01 escape mutants probably share the same epitope, the lethality of the two mutants the compared with that of the parental A/Shanghai H7N9 strain was quite different. The 045-051310-2B06 escape mutant was highly attenuated ($LD_{50} > 1.10^5$) compared with the wild-type A/Shanghai H7N9 strain ($LD_{50} = 4.6 \times 10^3$), and none of the mice succumbed to infection. In contrast, the S6-B01 escape mutant closely mimicked the parental strain, and all mice challenged with 100,000 PFU succumbed to infection. However, the LD_{50} of the S6-B01 mutant ($LD_{50} = 3.2 \times 10^4$) was still higher than that of the wild-type A/Shanghai H7N9 strain. The 042-100809-2F04 escape mutant was moderately attenuated ($LD_{50} = 5.2 \times 10^4$) (Figure 7). All together, these results demonstrate that escape from stalk-reactive antibodies may have a negative effect on virus fitness in vivo.

The loss of binding observed for 042-100809-2F04 is only mediated by escape mutations in the HA stalk domain. We demonstrated earlier that the phenotype of the 045-051310-2B06 escape mutant was dependent on the stalk mutations (complete loss of binding and loss of viral fitness). Our results also suggest that 045-051310-2B06 and S6-B01 bind to the same epitope on the stalk region. For the 042-100809-2F04 escape mutant, the loss of binding was more dramatic when the head and stalk mutations were combined. In addition, the pathogenicity of the escape mutant viruses was moderate. In order to confirm that the mutations in the stalk domain are responsible for antibody binding, we generated infectious reassortant viruses with individual head and stalk mutations. We used immunofluorescence to characterize antibody binding to four 042-100809-2F04 point mutant viruses: R364K (stalk mutation), G63E/G234D (head mutations), G63E, and G234D. 042-100809-2F04 bound to the wild-type A/Shanghai H7N9 virus and to all combinations of the head domain mutation reassortants (G63E/G234D,

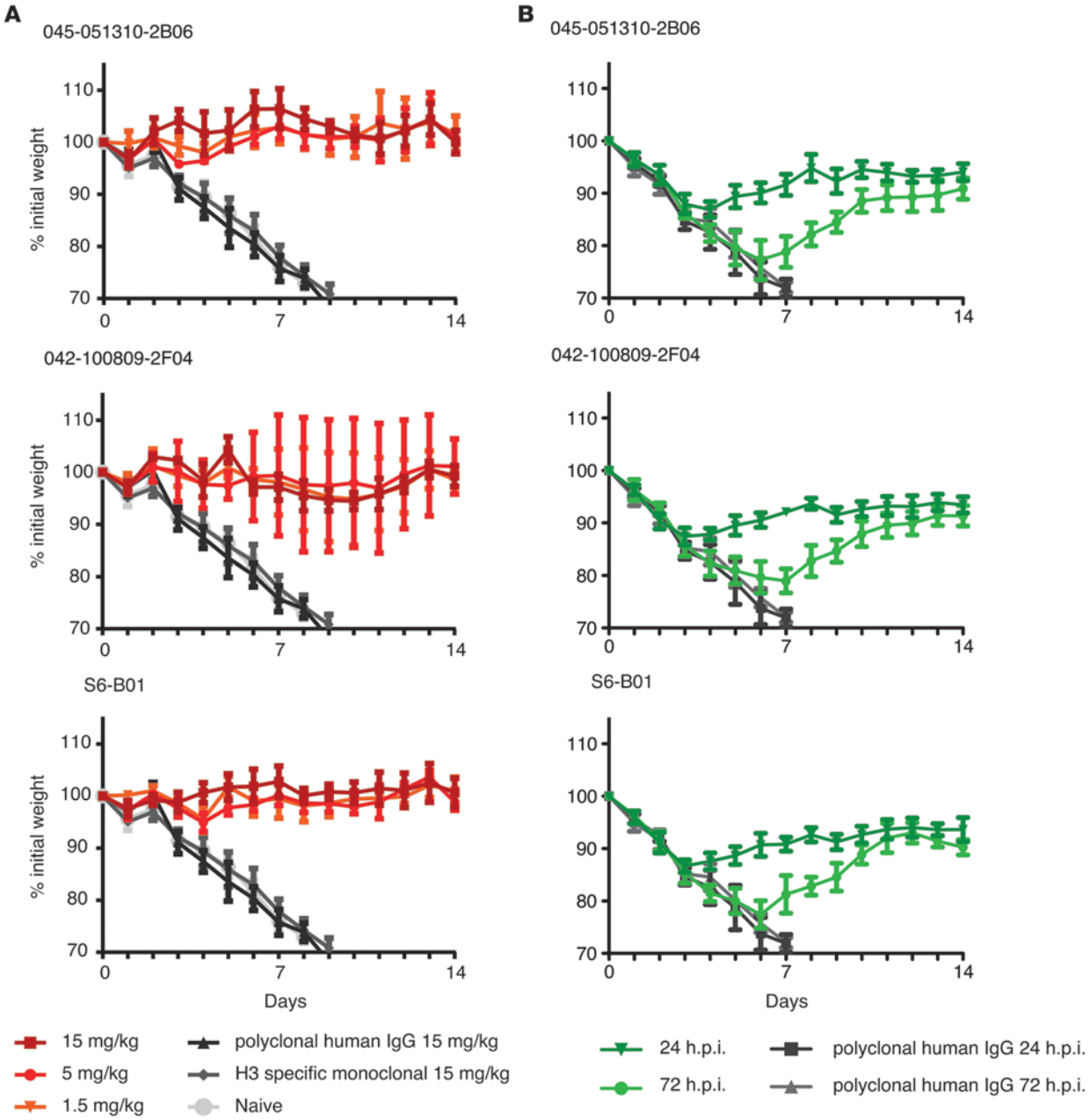

Figure 2. Passive transfer of the H7N9-neutralizing antibodies in mice. (**A**) 6- to 8-week-old female BALB/c mice (5 per experimental condition) were injected intraperitoneally with 1.5, 5, or 15 mg/kg of antibody (045-051310-2B06, 042-100809-2F04, or S6-B01) and then infected with a lethal dose (7.5 LD_{50}) of A/Shanghai/1/2013 virus. The percentage of initial body weight (mean ± SEM) was plotted for each antibody and compared with untreated mice, mice that received 15 mg/kg of a polyclonal human IgG antibody, and mice that received 15 mg/kg 011-10069 2C01 (H3N2-neutralizing antibody). Control groups are the same for all 3 panels. (**B**) 6- to 8-week-old female BALB/c mice (5 per experimental condition) were infected with a lethal dose (7.5 LD_{50}) of A/Shanghai/1/2013 virus and then injected intraperitoneally with 15 mg/kg of antibody 24 or 72 hours after infection. The percentage of initial body weight (mean ± SEM) was plotted for each antibody and compared with untreated mice and mice that received 15 mg/kg of a polyclonal human IgG antibody. Control groups are the same for all 3 panels. h.p.i., hours postinfection.

G63E, and G234D). As expected, binding to the stalk escape mutant (R364K) was lost as well as binding to the control full escape mutant (G63E/G234D/R364K) (Figure 8A).

To further characterize these point mutant viruses, we observed viral replication under the presence of antibody pressure (042-100809-2F04) in vitro via a microneutralization assay. In line with our previous results, the full 042-100809-2F04 escape mutant (G63E/G234D/R364K) evaded antibody neutralization as well as virus with the stalk mutation alone (R364K). In contrast, all combinations of mutations on the head domain failed to evade antibody neutralization. As expected, 042-100809-2F04 neutralized the wild-type A/Shanghai H7N9 virus (Figure 8B). These results confirm that the binding site of 042-100809-2F04 is on the HA stalk domain.

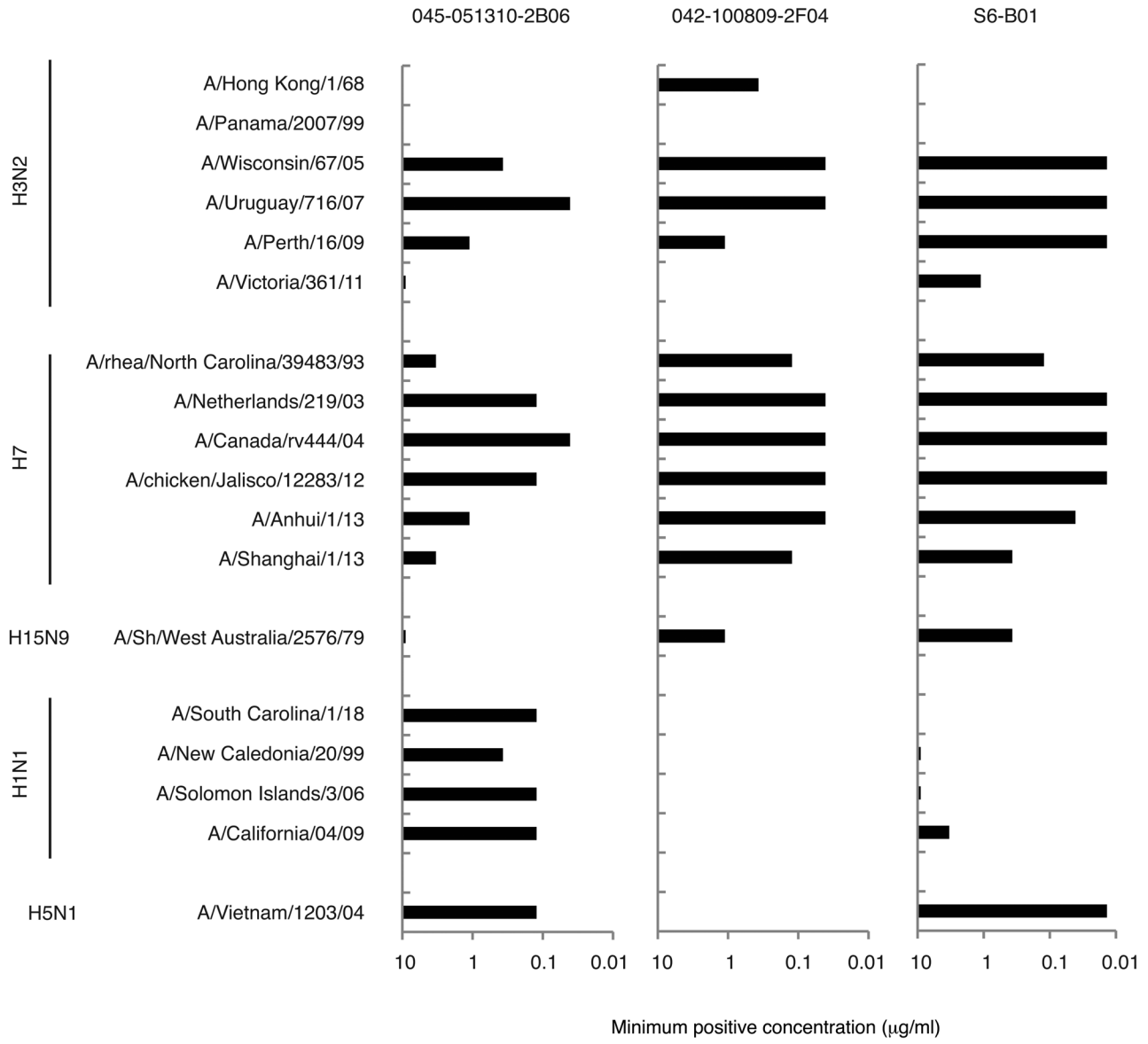

Figure 3. Virus strain cross-reactivity of the H7N9-neutralizing antibodies. Binding of the antibodies to multiple influenza A recombinant HA proteins from group 2 (H3N2 and H7) and group 1 (H1N1 and H5N1) was assessed by ELISA. The minimum positive concentration was defined as two standard deviations above the mean binding of randomly chosen naive B cell antibodies, as previously described (16). Data are representative of 3 independent experiments.

Discussion

Here, we report the use of an antibody microarray and subsequent functional assays to identify and characterize 3 antibodies that neutralize the emerging H7N9 influenza virus strain and protect mice from infection. These findings have several important implications. First, we demonstrate that H7 cross-reactive antibodies induced by vaccination with H1N1 or H3N2 influenza A strains are not uncommon. Previous studies have shown that broadly reactive antibodies binding to the HA stalk region are relatively rare (25), but they were preferentially induced by exposure to the highly unique 2009 pandemic H1N1 strain (16, 26, 27). It was hypothesized that exposure to this pandemic strain, which has a globular head domain that is highly divergent from prepandemic seasonal H1N1 strains, was activating cross-reactive memory B cells reactive with conserved epitopes (e.g., in the stalk region) that the virus shared with previous seasonal strains (2, 28). Indeed, one of the H7N9-neutralizing antibodies (045-051310-2B06) that we identified was induced by vaccination with this pandemic influenza strain. Importantly, the two other neutralizing antibodies, and the 3 H7 cross-reactive antibodies that bound without neutralizing activity, were primed by H3N2 seasonal strains. While it has been shown that H3N2 infection/vaccination can induce HA stalk-reactive antibodies, the design of these past studies could not predict the frequency at which the H3 stalk epitopes are targeted (29, 30). Our study demonstrates that group 2 cross-reactive antibodies are not uncommon following vaccination with seasonal H3N2 strains. Although the level of serum protection in the general population remains to be determined, our results suggest that prior immunity against the H7N9 strain and other novel strains could be boosted with a vaccine eliciting cross-reactive memory B cells. Indeed, as

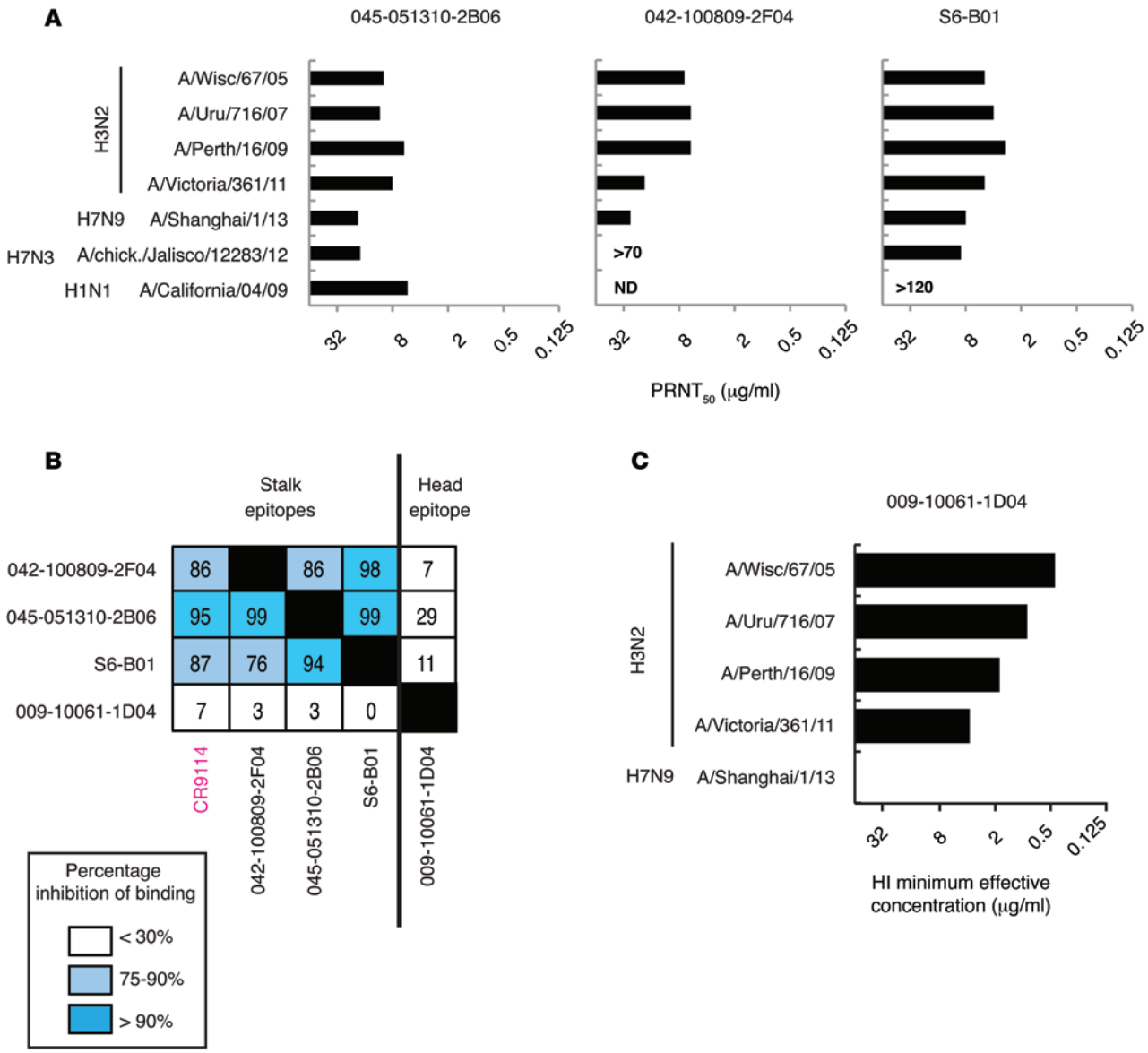

Figure 4. Functional analysis of the H7N9-neutralizing antibodies. (**A**) In vitro neutralization by plaque reduction assay. $PRNT_{50}$ values (μg/ml) are displayed. The data shown are means of 4 replicates (2 independent experiments). (**B**) Competition ELISA was used to confirm binding of the antibodies to epitopes either on the stalk or the globular head of HA. The percentage of competition of each antibody against the other neutralizing antibodies and the CR9114 antibody, using the A/Uruguay/716/2007 recombinant HA protein, is shown. The percentage here is the mean of 3 independent experiments. (**C**) Hemagglutination inhibition assay with various H3N2 strains and the H7N9 A/Shanghai/1/13 strain. Minimum effective concentration is shown (μg/ml), and results are displayed only for the antibody 009-10061-1D04, as the H7N9-neutralizing antibodies are negative on this assay. Data are representative of 3 independent experiments. HI, hemagglutination inhibition; ND, not determined.

recently demonstrated in mice, immunization with a chimeric HA protein expressing the H3 stalk domain induces broad protection against divergent H3N2 and H7 virus infection (31, 32). It will be important to determine whether booster immunizations with divergent influenza strains in the general human population can lead to universal protection against most influenza strains.

A better understanding of epitopes targeted by broadly neutralizing antibodies benefits the design and development of new influenza vaccines. It has been shown that neutralizing stalk-reactive antibodies are induced in relatively canonical responses encoded by the VH1-69 (19, 33) or the highly similar VH1-18 gene segments (26). In line with their similar binding and competition features, 045-051310-2B06 and S6-B01 are both encoded by the VH1-18 heavy chain variable gene segment (Supplemental Table 2), suggesting that these antibodies arose in a canonical response typical for binding to the HA stalk epitopes. Moreover, the escape viral mutations identified at residue 384 (I384N for 045-051310-2B06 and I384T for S6-B01) are located in the epitope targeted by the CR9114 antibody (VH1-69 gene segment), and the binding patterns of the antibodies (CR9114 and 045-051310-2B06; CR9114 and S6-B01) to the HA variants from escape mutants are identical. We hypothesize that these antibodies target the same or considerably overlapping

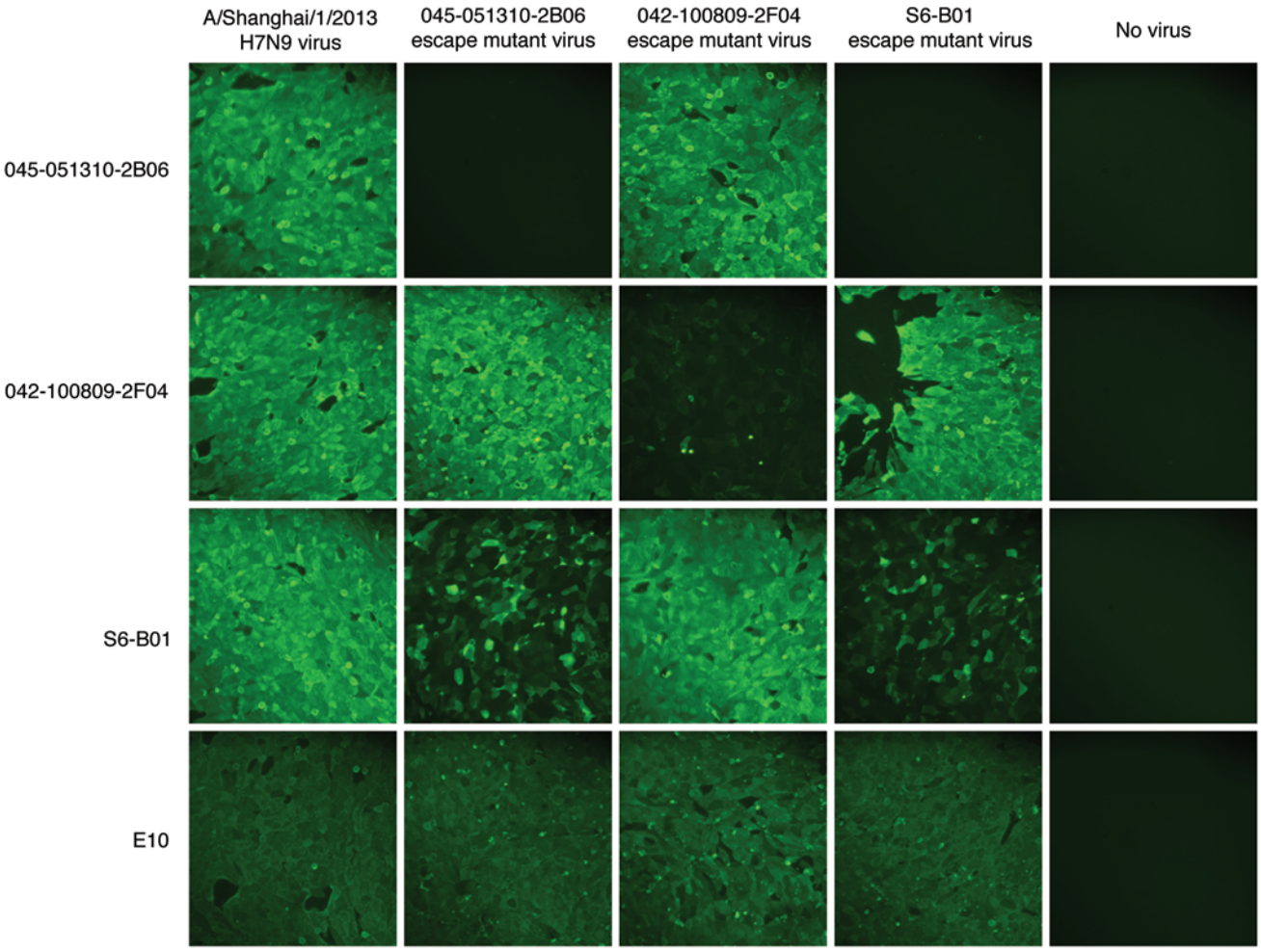

Figure 5. Binding analysis of escape mutants by immunofluorescence. MDCK cells were infected with the different escape mutant viruses (045-051310-2B06, 042-100809-2F04, or S6-B01) or the wild-type A/Shanghai/1/2013 virus and incubated with the neutralizing antibodies, individually, at 5 μg/ml. The infection was done in triplicate for each virus. A mouse anti-M2 protein antibody (E10) was used as a positive control of infection for each virus variants. Binding was visualized using an anti-IgG Alexa Fluor 488–conjugated antibody under an Olympus IX70 inverted fluorescence microscope. Original magnification, ×100.

epitopes on the stalk region. The differences in the sensitivity to epitope mutations between the two neutralizing antibodies could be explained by the fact that different antibodies have unique modes of binding. A recent study showed that a difference in the approach angle of an antibody to an HA stalk region could explain diversity in antibody potency (34). The antibody 042-100809-2F04 is encoded by VH3-23 (Supplemental Table 2). This antibody only binds and neutralizes group 2 strains and does not bind to the 045-051310-2B06 and S6-B01 escape mutants. Furthermore, the R364K mutation is located in the epitope targeted by the CR8020 antibody (23). In addition, 042-100809-2F04 has a similar binding pattern to HA variants as CR8020, suggesting that both antibodies have overlapping binding sites on the HA stalk region but target a different epitope than the group 1 and 2 broadly neutralizing antibodies.

The generation of escape mutants in our study led to interesting observations. First, the binding of the antibody S6-B01 to the escape mutant HA was not altered by the mutations occurring in the stalk region, despite viral escape and growth. To our knowledge, this is the first demonstration of viral escape without the ablation of antibody binding. This mechanism would provide a distinct selective advantage to the resulting virus, as B cell memory to this epitope would now be nonprotective, allowing immune evasion in an original antigenic sin fashion. Second, all 3 neutralizing viruses developed not only mutations in the stalk region but also amino acid substitutions in the globular head domain of HA. Due to the distance between the mutations in the stalk domain and these in the globular head domain, and the fact that the mutations in the stalk domain were sufficient to strongly interfere with binding to the HA, it is unlikely that the mutations in the globular head domain are directly affecting the binding of 042-100809-2F04, 045-051310-2B06, and S6-B01. By elucidating the binding requirements of 042-100809-2F04 in the context of an in vitro infection, we now demonstrate clearly that 042-100809-2F04 binds to the stalk domain, regardless of the head mutations. Instead, the globular head mutations could compensate for the loss of structural integrity caused by escape mutations in the stalk. This would suggest that escape from neutralization with stalk-reactive antibodies comes with a fitness loss for the virus, which we observed in mice for all 3 escape mutant viruses. In addition, these head

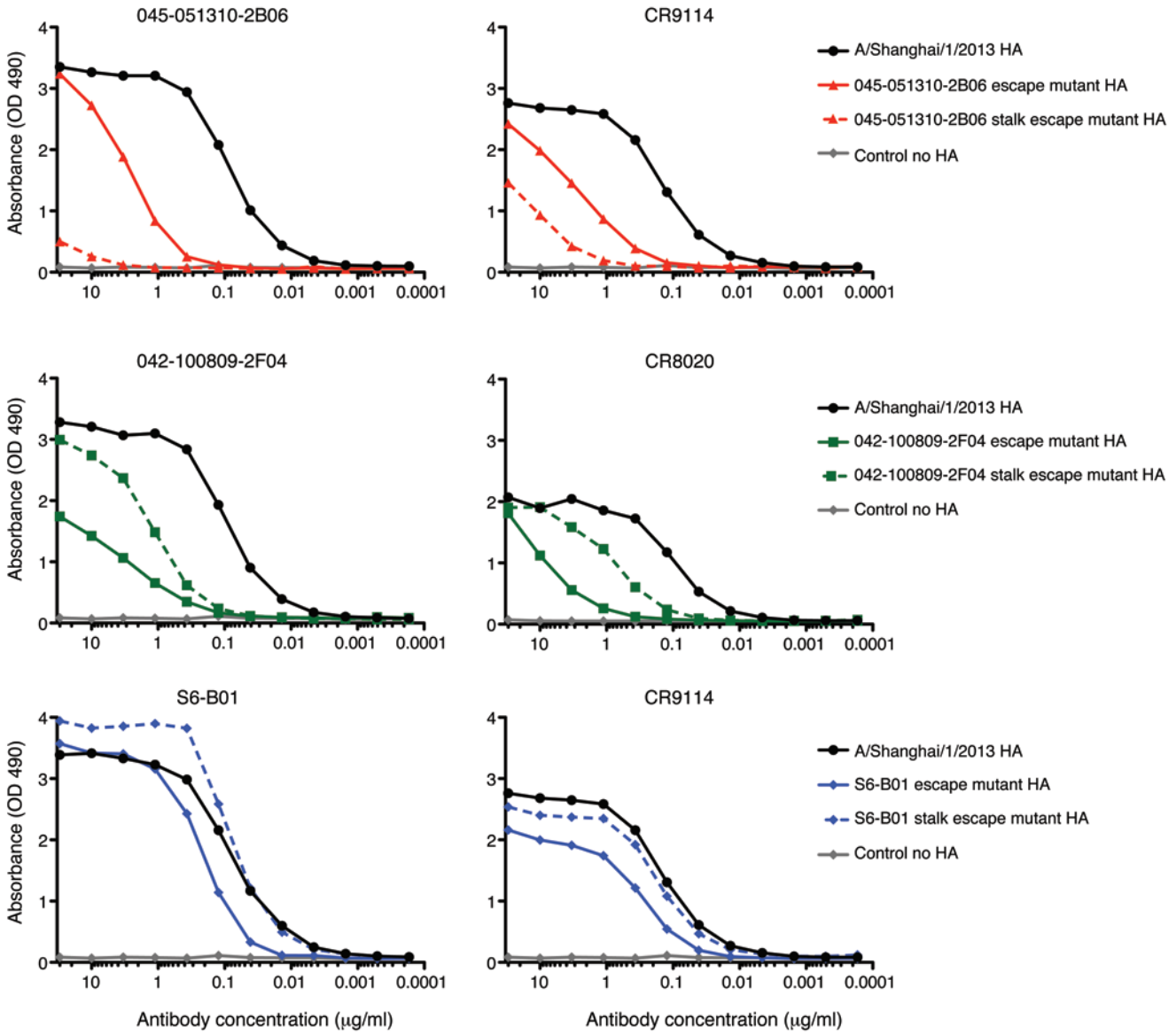

Figure 6. Binding analysis of the antibodies to recombinant HA escape mutants. Binding of the antibodies 045-051310-2B06, 042-100809-2F04, and S6-B01 to the corresponding HA mutants (both head and stalk mutations or stalk-only mutants) was assessed by ELISA. CR9114 and CR8020 antibodies were also tested against the mutant HAs. Absorbance was read at 490 nm. Reading above 3 is outside the linear range. The experiment was done in duplicate.

mutations might cause other effects, such as enhanced avidity to cellular receptors or increased structural stability, which could facilitate escape from neutralizing antibodies (35).

These studies emphasize the importance of receiving the annual influenza vaccine for protection against current circulating human influenza strains and future strains with pandemic potential. Identification of broadly neutralizing monoclonal antibodies is of major interest for therapeutic approaches, and many antibodies with conserved epitopes have been isolated from mice and humans (16, 19, 22, 33, 36–39). These various antibodies and the 3 H7N9-neutralizing antibodies reported here may prove useful to treat infections with emerging and pathogenic influenza strains. Future studies to evaluate the protective efficacy and safety of these antibodies in humans could lead to the next generation of prophylactic or therapeutic agents against influenza viruses.

Methods

Cells, viruses, and recombinant HA proteins. 293T and MDCK cells were obtained from the ATCC. H7N9 virus expressing the HA and NA of A/Shanghai/1/13 and the internal genes from A/Puerto Rico/8/34 was rescued as previously described (40). All influenza virus stocks used for the assays were freshly grown in SPF eggs, purified, and titered. Recombinant HA proteins derived from influenza A virus strains A/Uruguay/716/2007 (H3N2), A/Wisconsin/57/05 (H3N2), A/Perth/16/2009 (H3N2), A/Victoria/361/2011 (H3N2), A/Canada/rv444/2004 (H7N3), and A/Netherlands/219/2003 (H7N7) were obtained from BEI resources. Recombinant HA proteins derived from influenza A virus strains A/Panama/2007/99 (H3N2), A/Hong Kong/1/1968 (H3N2), A/chicken/Jalisco/12283/12 (H7N3), A/Anhui/1/13 (H7N9), A/Shanghai/1/13 (H7N9), A/rhea/North Carolina/39483/93 (H7N1), A/shearwater/West Australia/2576/79

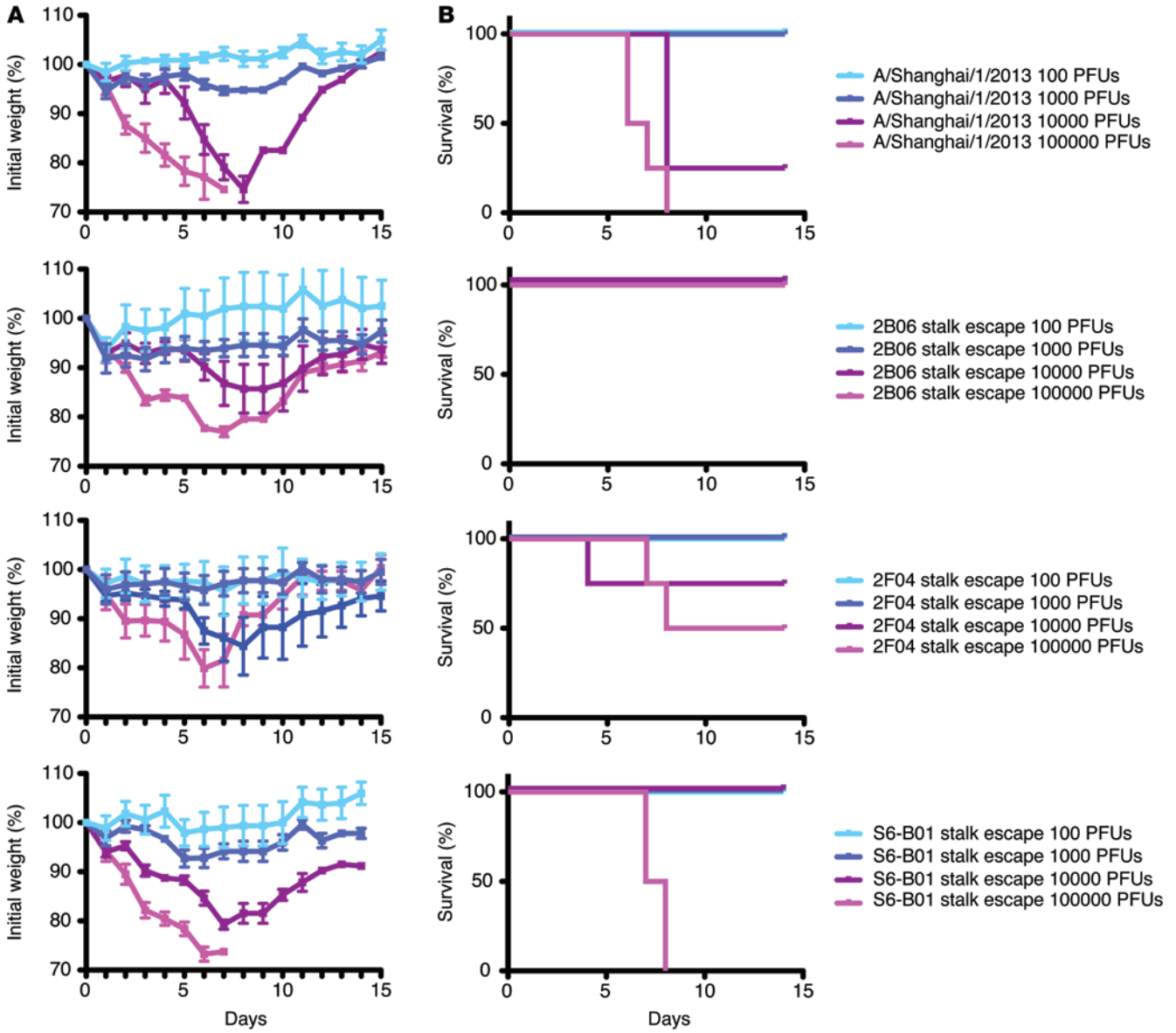

Figure 7. Pathogenicity of the stalk escape mutant viruses in vivo. 6- to 8-week-old female BALB/c mice (4 per experimental condition) were challenged with escalating doses, ranging from 100 to 100,000 PFU, of A/Shanghai/1/2013 H7N9 wild-type virus, 045-051310-2B06 stalk escape mutant virus, 042-100809-2F04 stalk escape mutant virus, or S6-B01 stalk escape mutant virus. (**A**) The percentage of initial body weight (mean ± SEM) and (**B**) the percentage survival (mean ± SEM) are plotted for each escape mutant.

(H15N9), A/California/04/09 (H1N1), and A/South Carolina/1/18 (H1N1) were expressed with a C-terminal trimerization domain and a hexahistidine tag in the baculovirus expression system as described before (41). A chimeric HA made of the stalk region of A/Shanghai/1/13 (H7N9), and the globular head domain of A/duck/Czechoslovakia/1956 (H4N6) was expressed as well using the same system (18).

Antibody microarray. Eighty-three H3N2-reactive antibodies were diluted in Protein Printing Buffer (ArrayIt) to 250 μg/ml and printed in triplicate on SuperEpoxy glass slides using the SpotBot 3 microarrayer (ArrayIt). Before use, slides were washed with PBS 0.05% Tween-20 and then treated with BlockIt blocking buffer (ArrayIt) for 1 hour at room temperature. Slides were washed 3 times with protein microarray wash buffer between each step, and all the reactions were done at room temperature in protein microarray reaction buffer (ArrayIt). To detect and normalize antibody signals, the slides were incubated for 1 hour with Cy3-conjugated goat anti-human IgG, Fc-fragment specific antibody (Jackson ImmunoResearch). Recombinant HA proteins were biotinylated with EZ-Link Maleimide-PEG2-Biotin (Pierce), and excess free biotin was removed using Zeba Desalting Columns (Pierce). Slides were incubated with 40 μg/ml of each recombinant HA for 1 hour and then with Alexa Fluor 647–conjugated Streptavidin (Invitrogen) for 1 hour. Signals were quantified using a GenePix 4000B microarray scanner and analyzed with GenePix Pro 6.0 software (Molecular Devices). Microarray data have been deposited in the MIAME-compliant GEO database (accession no. GSE63249 and GPL19411).

ELISA assays. Plates were coated with recombinant HAs at various concentrations depending on the HA (from 0.5 to 5 μg/ml) in PBS

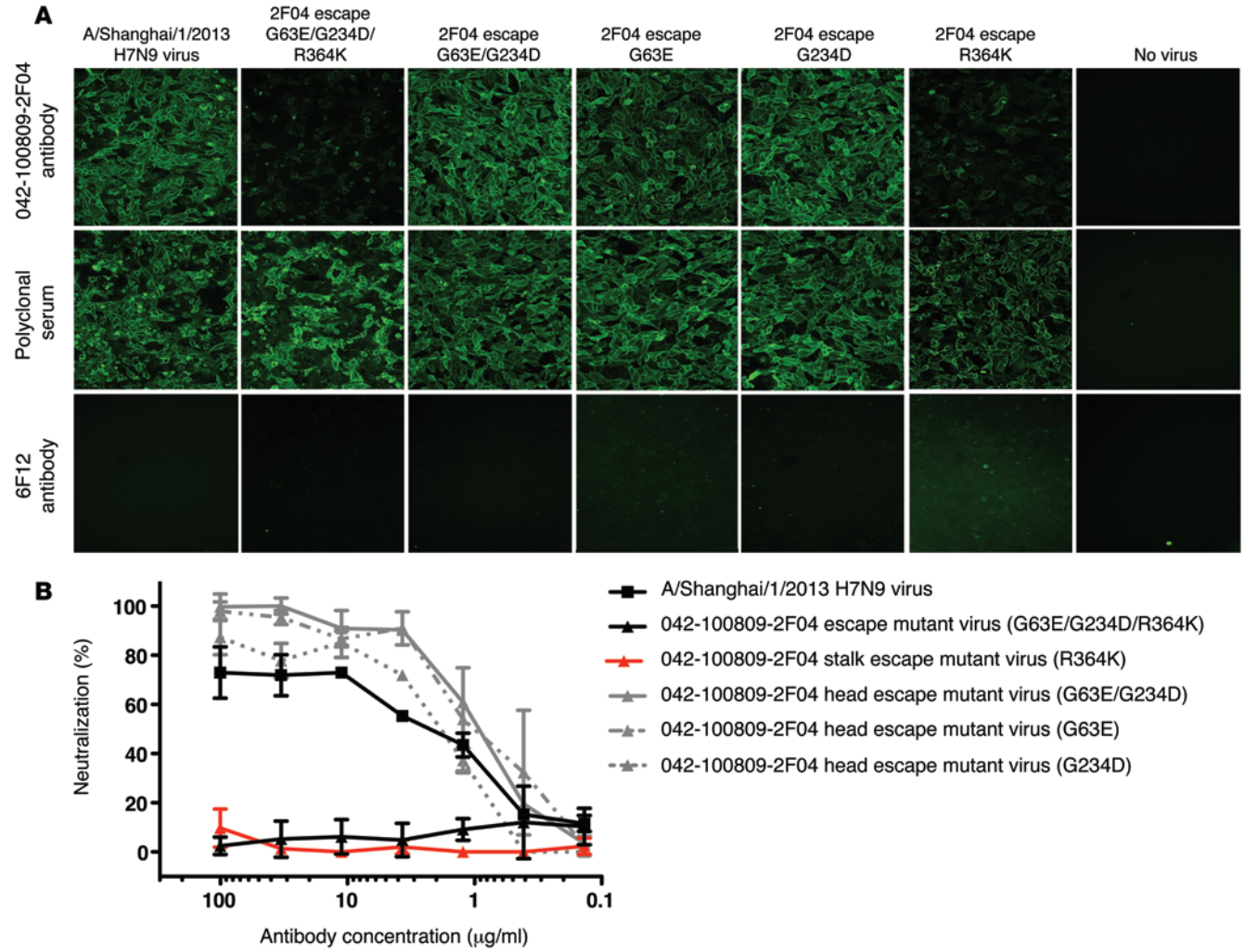

Figure 8. Characterization of point mutant escape viruses for the 042-100809-2F04 antibody. (**A**) Binding analysis of escape mutants by immunofluorescence. MDCK cells were infected with viruses containing different combinations of point mutations (R364K [stalk mutation], G63E/G234D [head mutations], G63E, and G234D), the full escape mutant (G63E/G234D/R364K), or the wild-type A/Shanghai/1/2013 virus and then incubated with 5 μg/ml 042-100809-2F04 antibody. The infection was done in triplicate for each virus. A polyclonal serum was used as a positive control of infection for each virus variant. The antibody 6F12 was used as a negative control. Binding was visualized using an anti-IgG Alexa Fluor 488–conjugated antibody under an Olympus IX70 inverted fluorescence microscope. Original magnification, ×100. (**B**) In vitro microneutralization assay using the 5 different escape mutant viruses generated for the 042-100809-2F04 antibody. A/Shanghai/1/2013 (H7N9) viruses were used as a control. The data shown are mean ± SEM of triplicates.

overnight at 4°C. After blocking, antibodies were incubated (starting concentration 10 μg/ml) for 1 hour at 37°C. HRP-conjugated goat anti-human IgG antibody (Jackson ImmunoResearch) was used to detect binding of the mAbs, followed by development with Super Aquablue ELISA substrate (eBiosciences). Absorbance was measured at 405 nm on a microplate spectrophotometer (Bio-Rad). To standardize the assays, high-affinity antibodies with known binding characteristics were included on each plate, and the plates were developed when the absorbance of these controls reached 3.0 ± 0.1 OD units.

Competition ELISAs were performed by inhibition of binding of each biotinylated antibody of interest at the half-maximal binding concentration with a 10-fold molar excess of competitor antibody. HRP-conjugated streptavidin (Southern Biotech) was used for detection. The absorbance value of each antibody against itself is scored at 100% inhibition, and comparison of different antibodies was done as a percentage of this 100% inhibition.

Memory B cell assay and ELISPOT. PBMCs were plated at 5×10^5 cells per well in media supplemented with pokeweed mitogen extract, phosphothiolated CpG ODN-2006 (Sigma-Aldrich), and *Staphylococcus aureus* Cowan (Sigma-Aldrich), as previously described (42). After 6 days, cells were washed and plated on 96-well filter plates (Millipore) coated with 2 μg/ml of various HAs. Cells were incubated overnight at 37°C, and plates were washed and then incubated with an anti-human IgG-biotin antibody (Mabtech), followed by streptavidin alkaline phosphatase (Southern Biotech). Plates were developed using NBT/BCIP (Thermo Scientific).

Hemagglutination inhibition assay. Viruses were diluted to 8 HA units per 50 μl, and 25 μl of virus was combined in duplicate wells with an equal volume of antibody serially diluted in PBS. 50 μl of 0.5% Turkey red blood cells (Lampire Biological) was then added and incubated for 1 hour at room temperature. Minimum effective concentrations were read based on the final dilution at which hemagglutination was observed.

Microneutralization assay. MDCK cells were maintained in minimum essential medium (MEM) supplemented with 10% fetal calf serum at 37°C. Three-fold serially diluted antibody (starting concentration 300 μg/ml) in serum-free MEM with TPCK-treated trypsin (Sigma-Aldrich) was mixed with an equal volume of virus (~1,000 $TCID_{50}$) and incubated 1 hour at 37°C. Confluent MDCK cells in 96-well format were washed twice with PBS, and the antibody/virus mixture was added to the cells and incubated for 1 hour at 37°C. Then the antibody/virus mixture was removed, and cells were cultured for 20 hours at 37°C with serum-free MEM containing TPCK-treated trypsin and the antibody at the appropriate concentration. Then cells were washed twice with PBS, fixed with 80% ice-cold acetone at –20°C for 1 hour, washed 3 times with PBS, blocked for 30 minutes with 5% milk-PBS, and then treated for 30 minutes with 2% H_2O_2. An anti-NP antibody (EVS) diluted in 3% BSA-PBS was incubated for 1 hour at room temperature. An HRP anti-mouse antibody (Santa Cruz Biotechnology) was used for detection, the plates were developed using SigmaFast OPD (Sigma-Aldrich), and the absorbance was measured at 490 nm. The final concentration of antibody that reduced infection to 50% (IC_{50}) was determined using GraphPad Prism software.

Plaque assay and $PRNT_{50}$ assay. Plaque assay was done as previously described (16), with the exception that cells were incubated for 48 hours with the agar overlay. Plaques were counted, and the final concentration of antibody that reduced plaques to 50% ($PRNT_{50}$) was determined using GraphPad Prism software.

Evaluation of the prophylactic and therapeutic efficacy in mice. Groups of 5 female BALB/c mice (The Jackson Laboratory) aged 6 to 8 weeks received a dose of 1.5, 5, or 15 mg/kg of purified antibody intraperitoneally. Control mice received purified human polyclonal IgG (Sigma-Aldrich) or a non-H7-binding H3N2-neutralizing monoclonal antibody (011-10069 2C01) at a 15 mg/kg dose. Two hours after treatment, mice were deeply anesthetized using a ketamine/xylazine mixture and infected with 7.5 LD_{50} (3,975 $TCID_{50}$) of A/Shanghai/1/2013 (H7N9) viruses diluted in PBS (pH 7.4). In a therapeutic setting, mice received a 15 mg/kg dose of each antibody individually 24 hours or 72 hours after infection. The mice were monitored daily for survival and weight loss until day 14 after infection. Animals that lost more than 25% of their initial body weight were euthanized.

Evaluation of the pathogenicity of the escape mutant viruses in mice and determination of the LD_{50}. Mice were challenged with escalating doses, ranging from 100 to 100,000 PFU, of the A/Shanghai/1/2013 H7N9 wild-type virus, the 045-051310-2B06 escape mutant virus, the 042-100809-2F04 escape mutant virus, or the S6-B01 escape mutant virus. The mice were monitored daily for survival and weight loss until day 14 after infection. Animals that lost more than 25% of their initial body weight were euthanized. The LD_{50} was determined using GraphPad Prism software.

Generation of escape mutants. A/Shanghai/1/2013 virus was diluted in serum-free MEM media and was incubated with MDCK cells in 24-well plates for 45 minutes. After the incubation, TPCK-treated trypsin-containing MEM media supplemented with antibody (045-051310-2B06, 042-100809-2F04, or S6-B01) at a concentration equivalent to 1 IC_{50} was added to the wells. Positive control wells (virus only) and negative control wells (no virus) were overlaid with TPCK-treated trypsin-containing MEM media only. Twenty-four hours after infection, supernatants were harvested and used to infect fresh cells that were again overlaid with TPCK-treated trypsin-containing MEM media, with or without 1 IC_{50} of the respective antibody. After 6 passages, the antibody concentration was increased to 2 IC_{50}. Three IC_{50} were used for passages 7 and 8. Viruses from passage 8 were plaque purified, and 4 clones of each virus were picked and grown in 10-day-old embryonated chicken eggs for 48 hours. The presence of virus was confirmed using an HA assay. RNA was extracted from allantoic fluid using TriZol reagent (Invitrogen), cDNA was generated using SuperScript III reverse transcriptase (Invitrogen), and HA segments were subjected to Sanger sequencing.

Generation of A/Shanghai/1/2013 with 042-100809-2F04 escape mutant point mutations. A/Shanghai/1/2013 wild-type virus was amplified with the following primers: TCGACCTCCGAAGTTGGGGGGGAGCAAAAGCAGGGGAAAATAAAAACAACCAAAATGAACACTCAAATCCTGGTATTCGCTCTGATTG (H7 HA forward) or TTTTGGGCCGCCGGGTTATTAGTAGAAACAAGGGTGTTTTTCCTCATATTTCTGAAATTCTAATCTTATATACAAATAGTGCACCGCATGTTTCCATTCT (H7 HA reverse). Point mutations, corresponding to 042-100809-2F04 escape mutant amino acid substitutions, were introduced to the A/Shanghai/1/2013 (H7N9) virus HA segment through site-directed mutagenesis via mutagenizing primers with regions of overlap. Alongside PCR fragments coding for 042-100809-2F04 point mutations, A/Shanghai/1/2013 wild-type PCR fragments were generated with similar primers lacking the nucleotide substitutions. PCR amplification with H7 HA forward and H7 HA reverse, along with combinations of these PCR fragments, allowed for generation of the 4 full-length HA segments, leading to the generation and isolation of the following gene segments: A/Shanghai/1/2013 HA R364K, A/Shanghai/1/2013 HA G63E/G234D, A/Shanghai/1/2013 HA G63E, and A/Shanghai/1/2013 HA G234D. The HA gene segments were then subcloned into the ambisense expression vector pDZ (43) via the In-Fusion HD Plus cloning Kit (Clontech). Virus was rescued via a reverse genetics system, as previously described (44, 45), with minor modifications to generate 6:2 reassortants (6 internal RNA segments from the influenza virus A/Puerto Rico/8/1934 and 2 genes encoding the HA and NA glycoproteins from A/Shanghai/1/2013). Individually, each pDZ plasmid coding for the HA segment was transfected with 7 other plasmids, coding for A/Shanghai/1/2013 NA and the remaining 6 segments from A/Puerto Rico/8/1934, into 293T cells. Twenty-four hours after transfection, supernatant/cell mixture was propagated in embryonated chicken eggs, as previously described. Rescued virus pools were dilution purified and sequence confirmed.

Immunofluorescence assay. MDCK cells were infected with A/Shanghai/1/2013 wild-type virus, the escape mutants (045-051310-2B06, 042-100809-2F04, or S6-B01 mutants), or with the single point mutation viruses (A/Shanghai/1/2013 HA R364K, A/Shanghai/1/2013 HA G63E/G234D, A/Shanghai/1/2013 HA G63E, or A/Shanghai/1/2013 HA G234D) at an MOI of 3 in the absence of trypsin overnight. The cell monolayer was fixed with PBS containing 0.5% paraformaldehyde for 30 minutes and then blocked with PBS containing 5% nonfat milk for another 30 minutes at room temperature. Monoclonal antibodies (045-051310-2B06, 042-100809-2F04, or S6-B01) were diluted to 5 μg/ml in PBS 1% BSA and incubated for 2 hours at room temperature. Cells were then washed 3 times with PBS. A goat anti-human IgG Alexa Fluor 488–conjugated antibody (Life Technologies Inc.) was used for detection. Binding was visualized using an Olympus IX70 inverted fluorescence microscope. The mouse mAb E10 (anti-M2 antibody, Center for Therapeutic Antibody Development at Icahn School of Medicine at

Mount Sinai) at 5 μg/ml or polyclonal serum from a serially H7-immunized mouse were used as a positive infection control, and a goat anti-mouse IgG Alexa Fluor 488–conjugated antibody (Life Technologies Inc.) was used for detection.

Expression of HA mutant recombinant proteins and binding analysis by ELISA. The HA segments of the escape mutants were cloned into baculovirus transfer vectors as described above. Additionally, hybrids with the head domain of the wild-type HA A/Shanghai/1/2013 and the stalk domains (demarcation line cysteines 52 and 277, H3 numbering) of the escape mutants were generated by PCR and cloned into baculovirus transfer vectors as well. HA proteins were then expressed as described above, and the binding of each antibody was assessed by ELISA using $Ni2^+$ plates (Qiagen). These plates were chosen specifically to ensure optimal structural integrity of the proteins. Briefly, plates were coated with recombinant HAs at 2 μg/ml in PBS overnight at 4°C. After blocking, antibodies were incubated (starting concentration 30 μg/ml) for 1 hour at 37°C. An HRP-labeled anti-human (Sigma-Aldrich) or HRP-labeled anti-mouse (Santa Cruz Biotechnology) antibody was used for detection, the plates were developed using SigmaFast OPD (Sigma-Aldrich), and the absorbance was measured at 490 nm.

Study approval. Monoclonal antibodies were generated as previously described (46) from individuals who had received seasonal influenza vaccination. Individuals were consented over the past 7 years for ongoing studies. These studies were performed with the approval of the Oklahoma Medical Research Foundation, Emory University, and The University of Chicago institutional review boards. All animal experiments were performed in accordance with and with approval of the Icahn School of Medicine at Mount Sinai Institutional Animal Care and Use Committee.

Acknowledgments

This work was supported in part by NIH grants 1U19AI08724 (to P.C. Wilson), HHSN272201400005C (to P.C. Wilson), 5U54AI057158 (to P.C. Wilson and R. Ahmed), 5U19AI057266 (to P.C. Wilson, R. Ahmed, and J. Wrammert), 1U19AI090023 (to P.C. Wilson, R. Ahmed, and J. Wrammert), 1P01AI097092 (to P.C. Wilson, R. Ahmed, P. Palese, and A. García-Sastre), and 1U19 AI109946 (to P.C. Wilson and P. Palese) and by funds provided by the Gwen Knapp Center for Lupus and Immunology Research. This work was also supported in part by CRIP (Center for Research on Influenza Pathogenesis), an NIAID-funded Center of Excellence for Influenza Research and Surveillance (contract HHSN272201400008C) (P. Palese, A. García-Sastre, F. Krammer). Florian Krammer was supported by an Erwin Schrödinger fellowship (J3232) from the Austrian Science Fund (FWF). Kaval Kaur was supported by a National Science Scholarship (PhD) from the Agency of Science, Technology and Research (A*STAR), Singapore. We thank Jori Reigle, Samuel Lim, Marissa Kumabe, Elizabeth Yan, and Lie Li for collecting blood samples; Meghan Sullivan, Noel Pauli, and Andrew Kinloch for helpful comments on the manuscript; and Ariana Hirsh for technical assistance.

Address correspondence to: Patrick C. Wilson, The University of Chicago, BSLC/Jules F. Knapp Building, 924 East 57th street, R414, Chicago, Illinois 60637, USA. Phone: 773.702.9009; E-mail: wilsonp@uchicago.edu. Or to: Florian Krammer, Department of Microbiology, Icahn School of Medicine at Mount Sinai, New York, New York 10029, USA. Phone: 212.241.7318; E-mail: florian.krammer@mssm.edu.

1. Shaw ML Palese P. Orthomyxoviruses. In: Knipe DM, Howley PM, eds. *Fields Virology*. 6th ed. Philadelphia, Pennsylvania, USA: Lippincott Williams and Wilkins; 2013:1151–1185.
2. Kaur K, Sullivan M, Wilson PC. Targeting B cell responses in universal influenza vaccine design. *Trends Immunol*. 2011;32(11):524–531.
3. Air GM. Sequence relationships among the hemagglutinin genes of 12 subtypes of influenza A virus. *Proc Natl Acad Sci U S A*. 1981;78(12):7639–7643.
4. Medina RA, Garcia-Sastre A. Influenza A viruses: new research developments. *Nat Rev Microbiol*. 2011;9(8):590–603.
5. Hirst M, et al. Novel avian influenza H7N3 strain outbreak, British Columbia. *Emerg Infect Dis*. 2004;10(12):2192–2195.
6. Fouchier RA, et al. Avian influenza A virus (H7N7) associated with human conjunctivitis and a fatal case of acute respiratory distress syndrome. *Proc Natl Acad Sci U S A*. 2004;101(5):1356–1361.
7. Gao R, et al. Human infection with a novel avian-origin influenza A (H7N9) virus. *N Engl J Med*. 2013;368(20):1888–1897.
8. Belser JA, et al. Pathogenesis transmission of avian influenza A (H7N9) virus in ferrets mice. *Nature*. 2013;501(7468):556–559.
9. Watanabe T, et al. Characterization of H7N9 influenza A viruses isolated from humans. *Nature*. 2013;501(7468):551–555.
10. Morens DM, Taubenberger JK, Fauci AS. H7N9 avian influenza A virus and the perpetual challenge of potential human pandemicity. *MBio*. 2013;4(4):1–14.
11. Hu Y, et al. Association between adverse clinical outcome in human disease caused by novel influenza A H7N9 virus and sustained viral shedding and emergence of antiviral resistance. *Lancet*. 2013;381(9885):2273–2279.
12. Zhang Q, et al. H7N9 influenza viruses are transmissible in ferrets by respiratory droplet. *Science*. 2013;341(6144):410–414.
13. Xu R, et al. Preferential recognition of avian-like receptors in human influenza A H7N9 viruses. *Science*. 2013;342(6163):1230–1235.
14. Ramos I, et al. H7N9 influenza viruses interact preferentially with α2,3-linked sialic acids and bind weakly to α2,6-linked sialic acids. *J Gen Virol*. 2013;94(pt 11):2417–2423.
15. Hai R, et al. Influenza A(H7N9) virus gains neuraminidase inhibitor resistance without loss of in vivo virulence or transmissibility. *Nat Commun*. 2013;4:2854.
16. Wrammert J, et al. Broadly cross-reactive antibodies dominate the human B cell response against 2009 pandemic H1N1 influenza virus infection. *J Exp Med*. 2011;208(1):181–193.
17. Wrammert J, et al. Rapid cloning of high-affinity human monoclonal antibodies against influenza virus. *Nature*. 2008;453(7195):667–671.
18. Krammer F, et al. An H7N1 influenza virus vaccine induces broadly reactive antibody responses against H7N9 in humans. *Clin Vaccine Immunol*. 2014;21(8):1153–1163.
19. Dreyfus C, et al. Highly conserved protective epitopes on influenza B viruses. *Science*. 2012;337(6100):1343–1348.
20. Kapczynski DR, et al. Characterization of the 2012 highly pathogenic avian influenza H7N3 virus isolated from poultry in an outbreak in Mexico: pathobiology and vaccine protection. *J Virol*. 2013;87(16):9086–9096.
21. Brandenburg B, et al. Mechanisms of hemagglutinin targeted influenza virus neutralization. *PLoS One*. 2013;8(12):e80034.
22. Tan GS, et al. Characterization of a broadly neutralizing monoclonal antibody that targets the fusion domain of group 2 influenza a virus hemagglutinin. *J Virol*. 2014;88(23):13580–13592.
23. Ekiert DC, et al. A highly conserved neutralizing epitope on group 2 influenza A viruses. *Science*. 2011;333(6044):843–850.
24. Hensley SE, et al. Hemagglutinin receptor binding avidity drives influenza A virus antigenic drift. *Science*. 2009;326(5953):734–736.
25. Corti D, et al. Heterosubtypic neutralizing antibodies are produced by individuals immunized with a seasonal influenza vaccine. *J Clin Invest*. 2010;120(5):1663–1673.
26. Li GM, et al. Pandemic H1N1 influenza vaccine induces a recall response in humans that favors broadly cross-reactive memory B cells. *Proc Natl Acad Sci U S A*. 2012;109(23):9047–9052.

27. Thomson CA, et al. Pandemic H1N1 influenza infection and vaccination in humans induces cross-protective antibodies that target the hemagglutinin stem. *Front Immunol*. 2012;3:87.
28. Wilson PC, Andrews SF. Tools to therapeutically harness the human antibody response. *Nat Rev Immunol*. 2012;12(10):709–719.
29. Ekiert DC, et al. Cross-neutralization of influenza A viruses mediated by a single antibody loop. *Nature*. 2012;489(7417):526–532.
30. Margine I, et al. H3N2 influenza virus infection induces broadly reactive hemagglutinin stalk antibodies in humans and mice. *J Virol*. 2013;87(8):4728–4737.
31. Margine I, et al. Hemagglutinin stalk-based universal vaccine constructs protect against group 2 influenza A viruses. *J Virol*. 2013;87(19):10435–10446.
32. Krammer F, et al. H3 stalk-based chimeric hemagglutinin influenza virus constructs protect mice from H7N9 challenge. *J Virol*. 2014;88(4):2340–2343.
33. Ekiert DC, et al. Antibody recognition of a highly conserved influenza virus epitope. *Science*. 2009;324(5924):246–251.
34. Friesen RH, et al. A common solution to group 2 influenza virus neutralization. *Proc Natl Acad Sci U S A*. 2014;111(1):445–450.
35. O'Donnell CD, et al. Antibody pressure by a human monoclonal antibody targeting the 2009 pandemic H1N1 virus hemagglutinin drives the emergence of a virus with increased virulence in mice. *MBio*. 2012;3(3):e00120-12.
36. Wang TT, et al. Broadly protective monoclonal antibodies against H3 influenza viruses following sequential immunization with different hemagglutinins. *PLoS Pathog*. 2010;6(2):e1000796.
37. Corti D, et al. A neutralizing antibody selected from plasma cells that binds to group 1 and group 2 influenza A hemagglutinins. *Science*. 2011;333(6044):850–856.
38. Throsby M, et al. Heterosubtypic neutralizing monoclonal antibodies cross-protective against H5N1 and H1N1 recovered from human IgM^+ memory B cells. *PLoS One*. 2008;3(12):e3942.
39. Sui J, et al. Structural and functional bases for broad-spectrum neutralization of avian and human influenza A viruses. *Nat Struct Mol Biol*. 2009;16(3):265–273.
40. Krammer F, et al. Divergent H7 immunogens offer protection from H7N9 virus challenge. *J Virol*. 2014;88(8):3976–3985.
41. Margine I, Palese P, Krammer F. Expression of functional recombinant hemagglutinin and neuraminidase proteins from the novel H7N9 influenza virus using the baculovirus expression system. *J Vis Exp*. 2013;(81):e51112.
42. Crotty S, Aubert RD, Glidewell J, Ahmed R. Tracking human antigen-specific memory B cells: a sensitive and generalized ELISPOT system. *J Immunol Methods*. 2004;286(1-2):111–122.
43. Quinlivan M, Zamarin D, Garcia-Sastre A, Cullinane A, Chambers T, Palese P. Attenuation of equine influenza viruses through truncations of the NS1 protein. *J Virol*. 2005;79(13):8431–8439.
44. Fodor E, Devenish L, Engelhardt OG, Palese P, Brownlee GG, Garcia-Sastre A. Rescue of influenza A virus from recombinant DNA. *J Virol*. 1999;73(11):9679–9682.
45. Hai R, et al. Influenza viruses expressing chimeric hemagglutinins: globular head and stalk domains derived from different subtypes. *J Virol*. 2012;86(10):5774–5781.
46. Smith K, et al. Rapid generation of fully human monoclonal antibodies specific to a vaccinating antigen. *Nat Protoc*. 2009;4(3):372–384.